Evidence for Processivity and Two-Step Binding of the RNA Substrate from Studies of J1/2 Mutants of the *Tetrahymena* Ribozyme[†]

Daniel Herschlag

Department of Chemistry and Biochemistry, Howard Hughes Medical Institute, University of Colorado, Boulder, Colorado 80309-0215

ABSTRACT: J1/2 of the *Tetrahymena* ribozyme, a sequence of three A residues, connects the RNA-binding site to the catalytic core. Addition or deletion of bases from J1/2 improves turnover and substrate specificity in the site-specific endonuclease reaction catalyzed by this ribozyme: $G_2CCCUCUA_5$ (S) + G $\rightleftharpoons$ $G_2CCCUCU$ (P) + GA_5. These paradoxical enhancements are caused by decreased affinity of the ribozyme for S and P [Young, B., Herschlag, D., & Cech, T. R. (1991) *Cell 67*, 1007]. An additional property of these mutant ribozymes, decreased fidelity of RNA cleavage, is now analyzed. (Fidelity is the ability to cleave at the correct phosphodiester bond within a particular RNA substrate.) Introduction of deoxy residues to give "chimeric" ribo/deoxyribooligonucleotides changes the positions of incorrect cleavage. Previous work indicated that S is bound to the ribozyme by both base pairing and tertiary interactions involving 2'-hydroxyl groups of S. The data herein strongly suggest that the P1 duplex, which consists of S base-paired with the 5' exon binding site of the ribozyme, can dock into tertiary interactions in different registers; different 2'-hydroxyl groups of S plug into tertiary contacts with the ribozyme in the different registers. It is concluded that the mutations decrease fidelity by increasing the probability of docking out of register relative to docking in the normal register, thereby giving cleavage at different positions along S. These data also show that the contribution of J1/2 to the tertiary interactions is indirect, not direct. Thus, a structural role of the nonconserved J1/2 is indicated: this sequence positions S to optimize tertiary binding interactions and to ensure cleavage at the phosphodiester bond corresponding to the 5' splice site. Substitution of sulfur for the nonbridging *pro-R*$_P$ oxygen atom at the normal cleavage site has no effect on $(k_{cat}/K_m)^S$ but decreases the fraction of cleavage at the normal site in reactions catalyzed by the −3A mutant ribozyme, which has all three A residues of J1/2 removed. Thus, the ribozyme chooses where to cleave S *after* rate-limiting binding of S, indicating that docking can change after binding and suggesting that the ribozyme could act processively. Indeed, it is shown that the +2A ribozyme cleaves at one position along an RNA substrate and then, before releasing that RNA product, cleaves it again. The ability of the substrate helix to move from one binding register to another without dissociation leads to a two-step model for RNA binding to the ribozyme: an "open" complex, in which S is held only by base-pairing interactions, precedes a "closed" complex, in which the base-paired duplex is docked into tertiary interactions. The change from the open to the closed complex can be described as an induced-fit conformational change, one which is able to contribute to specificity.

The intron from *Tetrahymena* pre-rRNA excises itself in the absence of proteins or self-splices, as do several related group I introns (Kruger et al., 1982; Cech, 1990). Circularization of the excised intron showed that catalytic activity is contained within the intron (Zaug et al., 1983), and conversion of this intramolecular self-splicing reaction into an intermolecular reaction catalyzed by a shortened form of the intron, or "ribozyme", has facilitated detailed investigations (Zaug & Cech, 1986; Zaug et al., 1988; McSwiggen & Cech, 1989; Herschlag & Cech, 1990a–c; Pyle et al., 1990; Herschlag et al., 1991). The site-specific endonuclease reaction catalyzed by the ribozyme is analogous to the first step of splicing, with the 5' splice site provided in trans (Figure 1).

J1/2 connects the 5' exon binding site of the ribozyme to the rest of the ribozyme (Figure 2). Even though J1/2 is not conserved in length or sequence among group I introns, mutations in this region have dramatic effects. These mutations (described in the right panel of Figure 2) decrease the binding of RNA oligonucleotides to the 5' exon binding site by up to 1000-fold but have little or no effect on the binding of DNA oligonucleotides (Young et al., 1991). These and other data provide evidence for tertiary interactions with 2'-hydroxyls of the oligonucleotide that stabilize that P1 duplex between substrate or product RNA oligonucleotides and the 5' exon binding site of the ribozyme [Figure 1 (bottom) and 2 (left); Sugimoto et al., 1989a; Herschlag & Cech, 1990a–c; Pyle et al., 1990; Pyle & Cech, 1991]. The differential effect of J1/2 on RNA and DNA binding suggests that J1/2 plays a role in these tertiary interactions that help stabilize the binding of RNA (Young et al., 1991).

Paradoxically, these mutations, which weaken binding, make the ribozyme a better enzyme. For the wild-type ribozyme, turnover with saturating RNA substrate is limited by slow dissociation of the second product in Figure 1 (bottom), $G_2CCCUCU$ (Herschlag & Cech, 1990b); the weaker binding to the mutant ribozymes speeds this rate-limiting step up to ~60-fold (Young et al., 1991). The wild-type ribozyme has very low specificity because essentially every RNA substrate molecule that binds is cleaved, whether the substrate forms a matched or mismatched duplex with the 5' exon binding site (Herschlag & Cech, 1990c); the weaker binding to the mutant
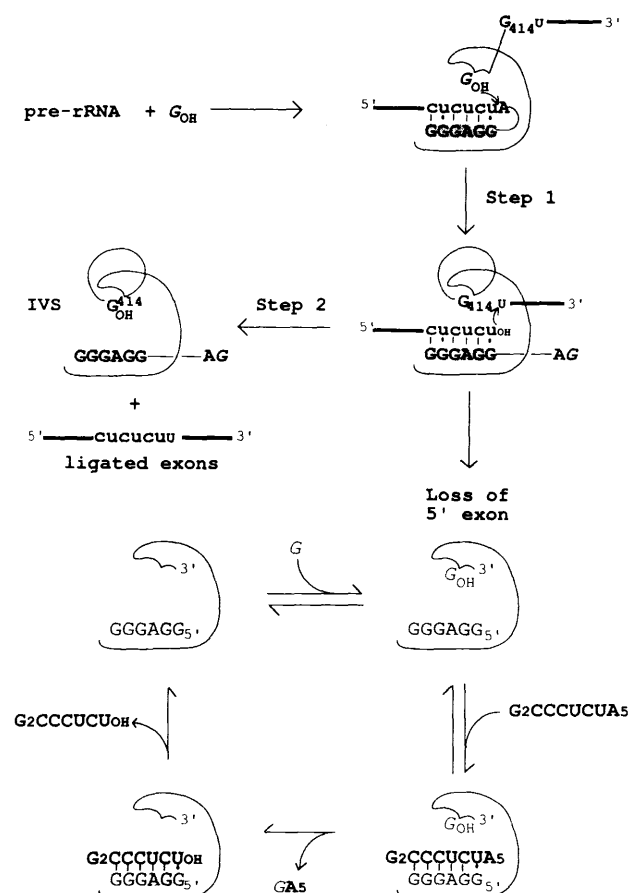
FIGURE 1: Comparison of the self-splicing (top) and endonuclease (bottom) reactions catalyzed by the *Tetrahymena* group I intron. (Top) The self-splicing reaction proceeds via two transesterification steps. After step 1 the 5' exon is no longer covalently attached so that it can, in principle, dissociate (loss of 5' exon) or proceed with step 2 to give ligated exons. (Bottom) Oligonucleotide substrates are cleaved by the L-21 *ScaI* ribozyme, a shortened version of the *Tetrahymena* intron RNA (Zaug et al., 1988). The reaction is analogous to the first step in self-splicing. This ribozyme has been engineered so that the sites of intramolecular cleavage and the 3'-terminal G_{414}, which can act as a nucleophile, are absent (Cech & Bass, 1986). Small letters denote the exons, capital letters denote the intron, italic G represents exogenous guanosine or GTP, and the shaded region is the 5' exon binding site, which forms the P1 helix with the 5' exon (top) or oligonucleotide (bottom). Reprinted with permission from Herschlag & Cech (1990a). Copyright 1990 Macmillan Journals.

ribozymes causes the mismatched substrate to dissociate prior to cleavage so that specificity is enhanced by up to ~70-fold (Young et al., 1991). The J1/2 mutations also decrease the fidelity of the site-specific endonuclease reaction. ("Fidelity" refers to the ability to cleave a substrate at the correct phosphodiester bond, that corresponding to the 5' splice junction.) Decreased fidelity in self-splicing would result in inaccurate ligation of exons in self-splicing (Young et al., 1991).

The infidelity caused by the J1/2 mutations is characterized herein and its physical basis explored. We find that the alternative cleavages arise from the P1 helix "docking" into the tertiary interactions in different registers. The ability to dock in different registers and a two-step binding process, in which docking is a step separate from formation of the base-paired duplex, allow the ribozyme to act processively.

MATERIALS AND METHODS

Materials. Unlabeled nucleoside triphosphates were purchased from P-L Biochemicals, guanosine from Sigma, [γ-^{32}P]ATP, [5'-^{32}P]cytidine 3',5'-bis(phosphate), [α-^{32}P]cor-

The L-21 *ScaI* wild-type and mutant ribozymes were prepared as described previously (Zaug et al., 1988; Young et al., 1991). The mutant ribozymes were kindly provided by B. Young. The oligonucleotides pppG$_2$CCCUCUAGU and (R_P)-pppG$_2$CCCUCU$_{(P-S)}$AGU[1] (i.e., with two nonbridging phosphoryl oxygen atoms and with one sulfur atom and one oxygen atom, respectively, at the UA phosphodiester linkage) were transcribed from a synthetic DNA template with T7 RNA polymerase using ATP or (S_P)-ATPαS and were a gift from J. McSwiggen (McSwiggen & Cech, 1989). The oligonucleotides pppG$_2$CCCUCUA$_5$ and pppG$_2$CCCUCU were also synthesized with T7 RNA polymerase in reaction mixtures with and without ATP, respectively, as described previously (Zaug et al., 1988). CCCUCU was made from pppG$_2$CCCUCU by treatment with RNase T1. The RNA oligonucleotide CCCCUCU and the mixed ribo/deoxyribo-oligonucleotides d4P, d5P, and d4,5P (defined in Scheme II below; Pyle & Cech, 1991) were made by solid-phase synthesis on an Applied Biosystems 380B DNA synthesizer with deprotection in ethanol/30% NH$_4$OH (3:1) overnight at 55 °C, followed by removal of the silyl protecting group by treatment with tetrabutylammonium fluoride in THF overnight at room temperature [see, e.g., Wu et al. (1989) and Scaringe et al. (1990)]. CCCU$_{(P-S)}$CUA$_5$ (mixed R_P and S_P isomers) was also made by solid-phase synthesis but with sulfur used in the oxidation of the UC phosphite to the phosphorothioate and was a gift from J. A. Piccirilli and A. Ritter.

RNA was 5'-end-labeled by treatment with calf alkaline phosphatase (only necessary for the oligonucleotides synthesized by transcription, not by solid-phase synthesis) followed by T4 polynucleotide kinase and [γ-^{32}P]ATP, as described previously (Zaug et al., 1988), except that the labeled oligonucleotides were used in kinetic experiments directly following elution from a gel slice into 10 mM Tris/1 mM EDTA, pH 7.5, without ethanol precipitation. The alternative procedure has no effect on kinetic parameters.

RNA was 3'-end-labeled with [5'-^{32}P]cytidine 3',5'-bis(phosphate), catalyzed by T4 RNA ligase, or with [α-^{32}P]-cordycepin, catalyzed by poly(A) polymerase, essentially as described previously (Tanner & Cech, 1985; Latham et al., 1990), and purified by PAGE, as described above.

Kinetics. Unless otherwise stated, reactions were carried out at 50 °C in 50 mM NaMES, pH 7.0 [determined at 25 °C; pH 6.7 at 50 °C, calculated from Good et al., (1966)], and 10 mM MgCl$_2$, as described in Herschlag and Cech (1990a). Briefly, reactions were initiated by addition of the 5'-end-labeled oligonucleotide after a 15-min preincubation
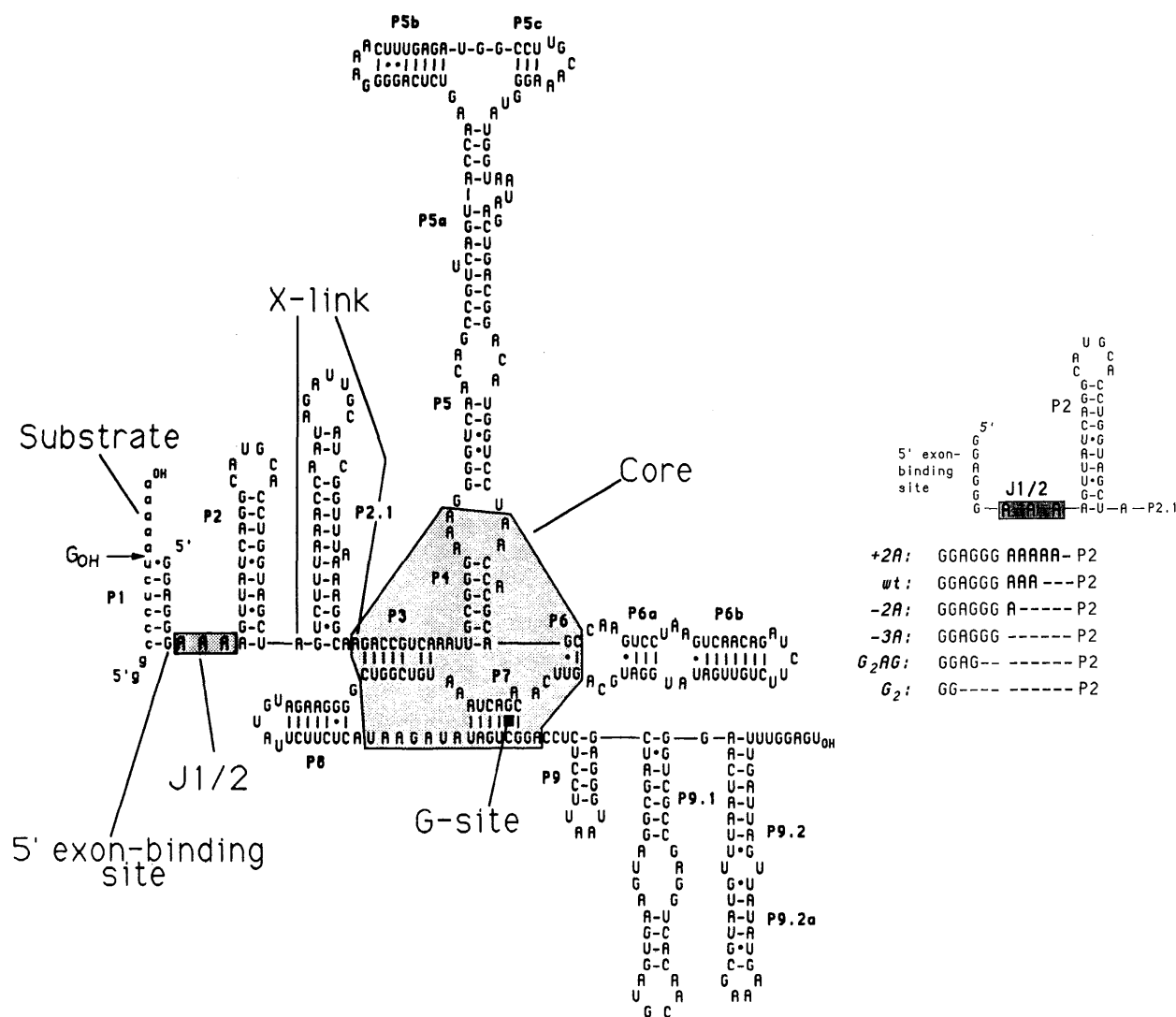
FIGURE 2: The sequence J1/2 in the wild-type and mutant ribozymes. (Left) The secondary structure of the wild-type L-21 *Sca*I ribozyme derived from the *Tetrahymena* intron. The RNA substrate (S) is shown in lower-case letters base-paired with the 5' exon binding site of the L-21 *Sca*I ribozyme to give the P1 duplex. "Core" is the catalytic core of the ribozyme, which includes the G-site in P7 that binds guanosine (Michel et al., 1989). "X-link" shows an efficient UV-induced cross-link (Downs & Cech, 1990). (Right) The secondary structure around J1/2, showing the wild-type and mutant J1/2 sequences. The names wt, +2A, -2A and -3A are used to refer to the wild-type and mutant ribozymes in the text. Reprinted with permission from Young et al. (1991). Copyright 1991 Cell Press.

of the ribozyme, MgCl₂, MES buffer, and guanosine at 50 °C. Typically about 6 aliquots of 1–2 μL were removed from 20-μL reaction mixtures at specified times and quenched with ~2 volumes of 20 mM EDTA in 90% formamide with 0.005% xylene cyanol, 0.01% bromophenol blue, and 1 mM Tris, pH 7.5. Product and substrate were separated by electrophoresis on 20% polyacrylamide/7 M urea gels, and their ratio at each time point was quantitated with use of an Ambis radioanalytic scanner. All reactions were single turnover, performed with an excess of ribozyme and only radiolabeled oligonucleotide reactant (~1 nM). Reactions were followed for ~3$t_{1/2}$, except for very slow reactions (e.g., reaction of the wild-type ribozyme with P*). Disappearance of the radiolabeled reactant was first order over the entire time course, with end points of ~95%, which corresponds to ~5% unreactive starting material. The slower reactions were followed for up to 180 min, and there was no evidence for curvature from inactivation of the ribozyme over this time.

Reaction of CCCU$_{(P-S)}$*CU.* CCCU$_{(P-S)}$CU (mixed R_P and S_P isomers) was generated in situ from CCCU$_{(P-S)}$CUA₅. Single-turnover reactions were carried out with 10 nM wt, +2A, or -2A ribozyme or 80 nM -3A ribozyme (Figure 2, right), 2.0 mM G, and ~1 nM 5'-end-labeled CCCU$_{(P-S)}$-

CUA₅. Almost all of this starting material was quickly converted to CCCU$_{(P-S)}$CU so that the slower cleavage of this oligonucleotide could be followed. The rate constants obtained are less precise for these reactions than for the others studied because the reactant was generated in situ and because there were two populations of reacting species, the R_P and S_P thioisomers.

RESULTS AND DISCUSSION

Fidelity Is Decreased by the Mutations in J1/2. The RNA endonuclease reaction of the *Tetrahymena* ribozyme is depicted in Figure 1 (bottom). The oligonucleotide substrate (S) is cleaved at the UpA bond, which corresponds to the 5' splice junction in the self-splicing reaction. However, in initial experiments with the J1/2 mutant ribozymes, shorter 5' products were also apparent (Young et al., 1991). Thus, these mutations decrease the *fidelity* of cleavage.
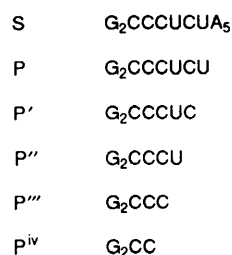
In order to study the alternate cleavages quantitatively, reactions were started with P, the normal product of the endonuclease reaction, rather than S, and the conversion of P to shorter products was followed (Scheme I). This is simpler than starting with S, as the additional products could come directly from cleavage of S or could arise from cleavage of

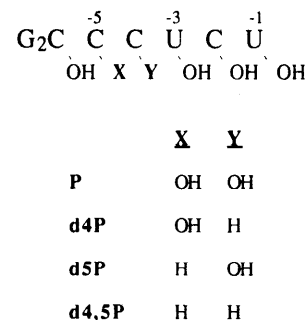Table I: Cleavage of P ($G_2CCCUCU$) by the Wild-Type and Mutant Ribozymes: Rates and Products[a]

ribozyme[b]	$J1/2^{b}$ A_n, $n=$	k_c^{P} [c] (min^{-1})	$K_d(E \cdot P)^{d}$ (nM)	$k_c^{P}/K_d(E \cdot P)$ (M^{-1} min^{-1})	k_c' [e] (min^{-1})	k_c'' [e] (min^{-1})	k_c''' [e] (min^{-1})	$k_c'/K_d(E \cdot P)$ (10^6 M^{-1} min^{-1})	$k_c''/K_d(E \cdot P)$ (10^6 M^{-1} min^{-1})	$k_c'''/K_d(E \cdot P)$ (10^6 M^{-1} min^{-1})
+2A	5	6[f]	15	4 × 10^8	0.3	5.6	0.1	20	370	7
wt	3	0.008[g]	1	8 × 10^6	0.0004	0.0076	<6 × 10^{-5}	0.4	8	<0.06
-2A	1	5[h]	150	3 × 10^7	<0.04	4.7	0.4	<0.3	30	3
-3A	0	4[i]	1000	4 × 10^6	0.9	3.0	0.1	0.9	3	0.1

[a] Reactions with 50 mM MES, pH 7, and 10 mM MgCl$_2$ at 50 °C. [b] The ribozymes and the J1/2 sequences are defined in Figure 2. [c] This rate constant represents that for the single-turnover reaction E·P*·G → products, i.e., with saturating ribozyme and G. The disappearance of P* to all products is followed, so that k_c^{P} is the sum of the rate constants for formation of the various products: $k_c^{P} = k_c' + k_c'' + k_c'''$. Reactions were carried out with 800 μM G, extrapolated to saturating G using $K_d(E \cdot G)$ = 1 mM for the wild-type ribozyme (Herschlag & Cech, 1990a) and $K_d(E \cdot G)$ = ~4 mM for the mutant ribozymes [estimated in Young et al. (1991)]. Although the uncertainty in the value of $K_d(E \cdot G)$ for the mutant ribozymes leads to considerable uncertainty in the values of k_c^{P} for the mutant ribozymes, this uncertainty does not affect conclusions in the text. [d] Values for wild type are from Herschlag and Cech (1990b) and values for the mutants are from Young et al. (1991). [e] Rate constants k_c', k_c'', and k_c''' are for the formation of P', P'', and P''' (Scheme I), respectively, from E·P*·G in single-turnover reactions, determined from k_c^{P} (footnote c) and quantitation of the ratio of the products formed from P, as in Figure 3A. Note that the values of k_c'' are reasonably precise, since this is the major product. However, the values and k_c' and k_c''' are considerably less precise since they are based upon quantitation of minor products (except for k_c' for the -3A ribozyme, as there is a considerable amount of P' formed by this ribozyme). [f] Obtained with 200 nM ribozyme. Reactions with 4–200 nM ribozyme showed that 200 nM ribozyme is saturating. A similar value of k_c^{P}, within 2-fold, was calculated from k_{obsd} with 10 nM ribozyme and 2 mM G, using $K_d(E \cdot P)$ and $K_d(E \cdot G)$. [g] Obtained with 50 nM ribozyme. The same value of k_c^{P}, within 20%, was calculated from k_{obsd} with 10 nM ribozyme and 2 mM G. Reactions with 15–80 nM ribozyme gave the same values of k_{obsd}, showing that these concentrations of ribozyme are saturating. [h] Obtained with 600 nM ribozyme, extrapolated to saturation using $K_d(E \cdot P)$ = 150 nM. The same value of k_c^{P}, within 30%, was calculated from k_{obsd} obtained with 10 nM ribozyme and 2 mM G. [i] Obtained with 600 nM ribozyme, extrapolated to saturation using $K_d(E \cdot P)$ = 1000 nM.

Scheme I

S	$G_2CCCUCUA_5$
P	$G_2CCCUCU$
P'	G_2CCCUC
P''	G_2CCCU
P'''	G_2CCC
P^{iv}	G_2CC

Scheme II

$$G_2C \overset{-5}{C} \, C \, \overset{-3}{U} \, C \, \overset{-1}{U}$$
$$ OH \; X \; Y \; OH \; OH \; OH$$

	X	Y
P	OH	OH
d4P	OH	H
d5P	H	OH
d4,5P	H	H

P, following its formation from S. (Both routes occur, as is described below.) With saturating or near-saturating concentrations of the mutant ribozymes, P was quickly cleaved to shorter products, with its disappearance following good first-order behavior for more than 3 half-lives, but with saturating wild-type ribozyme the cleavage was much slower, so that only the initial rate of cleavage could be followed (data not shown). Quantitation of these data showed that fidelity is decreased ~600-fold for the mutant ribozymes relative to the wild type, as determined from the ratio of rate constants for the cleavage of bound P, $k_c^{P(mutant)}/k_c^{P(wt)}$ (Table I). [P, the *substrate* in these reactions, is the normal *product* of the endonuclease reaction, so that faster cleavage of P represents lower fidelity; the chemical step for correct cleavage of S to give P is the same, within ~2-fold, for the wild-type and mutant ribozymes (Young et al., 1991).] The products from cleavage of P are mapped in Figure 3A and quantitated in Table I. The predominant product is P'' (defined in Scheme I) with the wild-type and mutant ribozymes (P'' is formed with rate constant k_c''; Table I). However, the -3A mutant gives a large amount of P', whereas this is a minor product with the wild-type and +2A ribozymes and is not observed with the -2A ribozyme (k_c', Table I). The -2A ribozyme instead gives a significant amount of P''', which is a very minor product of the other mutant ribozymes and is not observed with the wild-type ribozyme (k_c''', Table I).

Is the decreased fidelity simply a side effect of disrupting the overall ribozyme structure, giving a less efficient and less precise catalyst? The small decrease of ~2-fold in the rate of cleavage of S at the correct position caused by the mutations (Young et al., 1991) contrasted with the large increase in the rate of cleavage at the incorrect positions (k_c^{P}, Table I) suggests a more subtle or localized change rather than an overall disruption. The next two sections analyze the physical basis underlying the decrease in fidelity.

What Is Responsible for Infidelity? Binding of the oligonucleotide S or P to the wild-type ribozyme is stabilized by tertiary interactions that involve the 2'-hydroxyls of the oligonucleotide (Sugimoto et al., 1989b; Herschlag & Cech, 1990a; Pyle & Cech, 1991). For example, a ribooligonucleotide binds ~10^4-fold stronger than a deoxyribooligonucleotide of the same sequence (50 °C, 10 mM MgCl$_2$; Herschlag & Cech, 1990a,b). Studies of chimeric oligonucleotides, which contain both ribo and deoxyribo residues, have shown that the 2'-hydroxyl at position -3 from the normal cleavage site is the most important tertiary binding interaction (numbering as in Scheme II; Pyle & Cech, 1991; D.H., C. Grosshans, & T. R. Cech, unpublished results). In this section, this tertiary interaction is used as a reference point to demonstrate and characterize the modes of association of the ribozyme with the oligonucleotide P that are responsible for the aberrant cleavage of P to shorter products.

Consider two models: (A) The P1 helix between the oligonucleotide (P) and the 5' exon binding site of the ribozyme (Figure 1) is held fixed by the tertiary interactions so that the aberrant cleavages arise from guanosine, in its binding site in the catalytic core (Michel et al., 1989), moving along the P1 helix to cleave at the different positions. The mutations would increase the alternative cleavage by favoring motion of the guanosine site with respect to P1, which remains fixed with respect to its tertiary interactions. (B) The other possibility is that P1 is not fixed with respect to its tertiary interactions. In this model the oligonucleotide moves, so that a different 2'-hydroxyl replaces that at the -3 position in this tertiary contact. The guanosine site could then remain fixed with respect to the tertiary contact.

In order to distinguish between these models, the alternative cleavages of the chimeric oligonucleotides depicted in Scheme
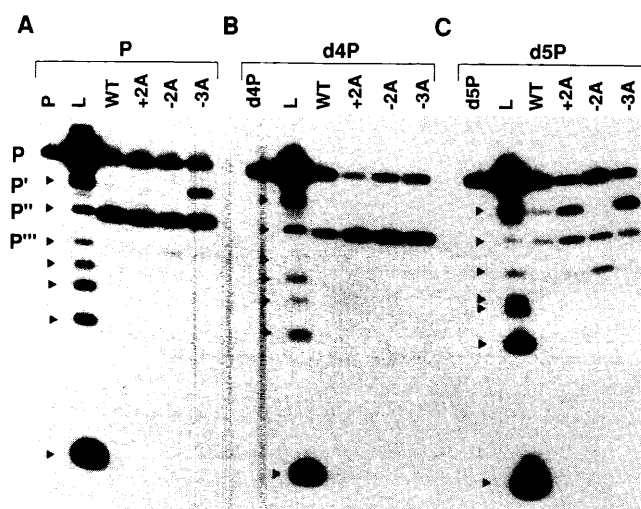
FIGURE 3: (A) Products of cleavage of P* (p*G₂CCCUCU) by the wild-type and mutant ribozymes. Lanes are as follows: P, P* starting material; L, ladder from partial digestion of P* by S1 nuclease, which leaves 3'-hydroxyls; wt, +2A, −2A, and −3A, single-turnover reactions of ~1 nM P* and 2.0 mM G with 10 nM wild-type ribozyme (180 min), 10 nM +2A ribozyme (2.5 min), 10 nM −2A ribozyme (10 min), and 80 nM −3A ribozyme (15 min), respectively. The ribozyme concentrations and incubation times were designed to give cleavage of slightly more than half of the P*, so that the products could be mapped. Thus, the rates of reaction of the different ribozymes cannot be conveniently compared in this figure; Table I contains such rate comparisons. The concentration of each ribozyme is kept constant in panels A, B and C, but the time of incubation is changed. (B) Products of cleavage of d4P* [p*G₂CC(dC)UCU] by the wild-type and mutant ribozymes. Lanes are analogous to those in panel A, as follows: d4P, d4P* starting material; L, ladder from partial digestion of d4P* by S1 nuclease; wt, +2A, −2A, and −3A, single-turnover reactions of ~1 nM d4P* and 2.0 mM G with 10 nM wild-type ribozyme (180 min), 10 nM +2A ribozyme (20 min), 10 nM −2A ribozyme (100 min), and 80 nM −3A ribozyme (100 min), respectively. A band across from the open arrow fifth from the bottom, corresponding to P‴, was visible in longer exposures. (C) Products of cleavage of d5P* [p*G₂C(dC)CUCU] by the wild-type and mutant ribozymes. Lanes are analogous to those in panel A, as follows: d5P, d5P* starting material; L, ladder from partial digestion of d5P* by P1 nuclease, which leaves 3'-hydroxyls; wt, +2A, −2A, and −3A, single-turnover reactions of ~1 nM P* and 2.0 mM G with 10 nM wild-type ribozyme (180 min), 10 nM +2A ribozyme (40 min), 10 nM −2A ribozyme (180 min), and 80 nM −3A ribozyme (100 min), respectively.

II were compared to the alternative cleavage of the all-ribo oligonucleotide, P. P″ is the predominant product from cleavage of P by the wild-type and mutant ribozymes (Figure 3A) but not from cleavage of d5P (Figure 3C).[2] Removal of the 2'-hydroxyl at the −5 position (i.e., d5P; Scheme II) is expected to greatly decrease formation of P″ if the tertiary interactions change (in accord with model B), because this 2'-hydroxyl is at position −3 relative to the P″ cleavage site. This change in cleavage position is quantitated in Table II. For cleavage of P by the wild-type, +2A, and −3A ribozymes, the ratio of [P']/[P″] is <1; however, for cleavage of d5P, there is a dramatic change in this ratio to ≥1 (Table IIA). Similarly, the ratio of [P‴]/[P″] for cleavage of P by the +2A, −2A, and −3A ribozymes is increased ~10-fold when d5P is the substrate (Table IIB). The observed change in the ratio of products cannot be accounted for by model A, in which the tertiary interaction remains constant regardless of the position of cleavage. Additional support for model B comes from the

Table II: Removal of the 2'-Hydroxyl Moiety at Position −4 or −5 of G₂CCCUCU (P) Changes the Distribution of Products of Cleavage Catalyzed by the Wild-Type and Mutant Ribozymes[a]

ribozyme	starting oligonucleotide		
	P	d5P	d4P
(A) Product Ratio [P']/[P″]			
wt	1/20	1.3	<1/10
+2A	1/20	1.5	<1/10
−3A	1/3	3.4	<1/40
(B) Product Ratio [P‴]/[P″]			
+2A	~1/50	1/5	<1/100
−2A	1/10	1	<1/100
−3A	~1/40	1/10	<1/100

[a] Reactions were carried out with 50 mM MES, pH 7, 10 mM MgCl₂, and 2.0 mM G at 50 °C, with ~1 nM of 5'-end-labeled oligonucleotide (P, d5P, and d4P are defined in Scheme II) and 10 nM of each ribozyme, except the −3A ribozyme, which was present at 10 or 80 nM in different reactions. P', P″ and P‴ are defined in Scheme I. The ratios are derived from initial rates to avoid secondary reactions of, for example, P' → P″. The uncertainty is substantial for the ratios that are far from 1 because the amount of a minor product had to be quantitated. This does not, however, obscure the qualitative trends described in the text. Data for the [P']/[P″] ratio for the −2A ribozyme and the [P‴]/[P″] ratio for the wild-type ribozyme are not included, because there was no measurable formation of P' by the −2A ribozyme or P‴ by the wild-type ribozyme.

Scheme III

reactions of d4P. P' is formed as a substantial product from the −3A ribozyme but is not formed to a detectable extent from d4P (Figure 3A,B; see also Table IIA). This is expected from model B since the 2'-hydroxyl at position −4 is three away from the P' cleavage site. The rate of formation of P″ from d4P is also decreased relative to its rate of formation from P (data not shown); this is again consistent with model B, as the 2'-hydroxyl of the nucleotide at position −2 relative to the cleavage site also has a significant effect on binding and cleavage in the normal site-specific endonuclease reaction (Pyle & Cech, 1991; D.H. & T. R. Cech, unpublished results). No cleavage of d4P to give P‴ was observed (Figure 3B; Table IIB). This is analogous to the large decrease in rate observed for the wild-type ribozyme when the 2'-hydroxyl at the cleavage site of the normal substrate is replaced by a 2'-hydrogen to give CCCUCdUA₅ (D.H., J. A. Piccirilli, & T. R. Cech, unpublished results). Finally, product ratios from reactions of d4,5P, which is missing the 2'-hydroxyl moieties at both position −4 and −5, change from those for reactions of d4P and d5P (data not shown), again consistent with movement of the tertiary interactions according to model B.

Even when J1/2 is completely removed to give the −3A ribozyme, recleavage of P is still affected by the 2'-hydroxyls at positions −3 and −2 from the cleavage site. This strongly suggests that the tertiary contacts are made with the residues outside of J1/2. However, the binding data presented by Young et al. (1991) show that J1/2 mutations affect the net binding energy that is obtained from the tertiary interactions. Thus, J1/2 plays a role in the tertiary interactions, but this role is indirect rather than direct (see Structure–Function Implications).

Is Infidelity Caused by Alternative Docking of the P1 Helix or Sliding of the Oligonucleotide along the 5' Exon Binding Site? The above comparison of the reactions of P, d5P, and d4P showed that their cleavage is accompanied by a change

---

[2] P″ with a deoxy residue at position −5 (i.e., d5P″; see Schemes I and II) is the actual product from reaction of d5P. For simplicity, the d5 and d4 notation is omitted in referring to the products of d5P and d4P cleavage.

Table III: Test of Docking versus Sliding Models by Comparison of Cleavage Rates for C_3UCU and C_4UCU^a

	k_{rel}^b		
ribozyme	C_3UCU	C_4UCU	$(G_2)C_3UCU$
wt	(1)	0.7	1.6
+2A	(1)	0.9	0.7
−2A	(1)	1.1	1.2
−3A	(1)	1.7	1.1

^{a} Reactions with 10 nM ribozyme, ~ 1 nM 5'-end-labeled oligo-nucleotide, and 2.0 mM G in the presence of 50 mM MES, pH 7, and 10 mM $MgCl_2$ at 50 °C. ^{b} Rate constants are relative to that observed for cleavage of C_3UCU; i.e., $k_{rel} = k_{obsd}^{oligo}/k_{obsd}^{C_3UCU}$. The ratio of products corresponding to cleavage at the positions giving P'' and P' (Table II and Scheme II) was the same, within 2-fold for the different oligonucleotides. However, there was an increase in the amount of the minor products corresponding to cleavage at the positions giving P''' and P^{IV} with C_4UCU (i.e., C_4 and C_3, respectively). In all cases C_4 and C_3 combined accounted for less than 30% of the total products.

in the position of the bound oligonucleotide such that the tertiary interactions are displaced 5' along the oligonucleotide. This could be accomplished in two ways: the P1 helix could "dock" with the tertiary contacts in a different register, or the oligonucleotide could "slide" along the 5' exon binding site, which is the other strand of P1, as depicted in Scheme III.

The docking and sliding models were tested by comparing the cleavage of CCCUCU and CCCCUCU. In the sliding model, rate of cleavage of CCCCUCU should be much greater than the rate of cleavage of CCCUCU, because the added C residue would give an additional G·C base pair, thereby favoring the alternative binding modes in Scheme III. In contrast, the added C residue is not expected to have a significant effect if the intact P1 helix docks in different registers, as the base pairing does not change in this model (Scheme III, left structure). The results in Table III show that the rate of cleavage of CCCUCU and CCCCUCU are similar, within 2-fold for each ribozyme. The rates of cleavage of CCCUCU and G_2CCCUCU are also similar (Table III), providing no indication of a 5' length effect that might otherwise interfere with this test.[3] Thus, the P1 helix moves as a unit, docking into the tertiary contacts in different registers and thereby allowing the oligonucleotide to be cleaved at additional sites.

With the P1 helix docking into the tertiary interactions in different registers, the simplest model for cleavage to give the shorter products is that the active site remains fixed with respect to the positions of tertiary contacts on the ribozyme. The following data suggest that this is indeed the case. (1) For the normal cleavage to give P, substitution of sulfur for a nonbridging phosphoryl oxygen atom to form the R_P thio isomer slows the chemical step 2-fold for the wild-type and mutant ribozymes (Herschlag et al., 1991; Young et al., 1991); substitution to give the S_P thio isomer slows the chemical step >1000-fold for the wild-type ribozyme, providing strong support for an interaction of the ribozyme (or a ribozyme-bound metal ion) with the *pro-S* oxygen atom (J. A. Piccirilli and T. R. Cech, unpublished results). $CCCU_{(P-S)}CU$ has a mixture of the R_P and S_P thio isomers at the position of cleavage that gives P''. Reactions of this oligonucleotide with the wild-type and mutant ribozymes are consistent with a small

---

[3] There is an increase in the fraction of shorter products from C_4UCU compared to the products from C_3UCU (Table III, footnote b). This presumably arises from an additional reaction pathway analogous to the C_5 cleavage reaction catalyzed by the ribozyme (Zaug & Cech, 1986). However, these shorter species remain minor products (<30%) so that the rate constants for cleavage of C_4UCU in Table III are not significantly altered by the additional reaction pathway and the conclusion is unaffected.

Scheme IV

A

B
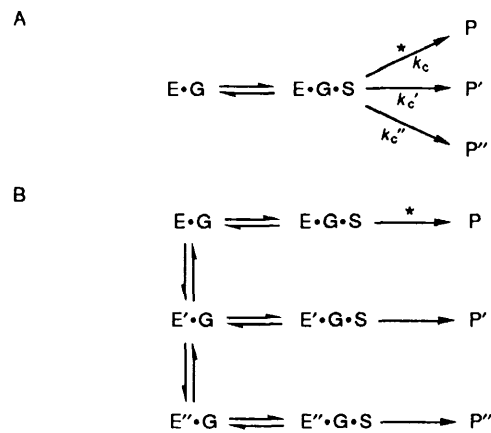
thio effect of $\sim$3-fold for half of the molecules, presumably the R_P thio isomer, and a much larger thio effect for the other half of the molecules, presumably the S_P thio isomer, so that about half of the products are P' and P''' instead of P'' (reactions as described under Materials and Methods; data not shown). These results suggest that the environment around the *pro-S* oxygen is the same during the unfaithful cleavage of P as it is in the normal cleavage of S. (2) The chemical step of the normal cleavage reaction of S by the wild-type ribozyme is approximately first order in [OH$^-$] from pH 5.2 to 7.0 (D.H. & T. R. Cech, unpublished results). The same pH dependence was observed for the cleavage of P. Analogous results were obtained for cleavage of S and P by the +2A ribozyme. In addition, the ratio of products from cleavage of P and from cleavage of d5P by the wild-type ribozyme was the same at pH 6.1 and 7.0 (data not shown). These results are consistent with the same overall mechanistic pathway and the same rate-limiting step in the aberrant cleavage of P as in the normal cleavage of S.

The decreased fidelity of the mutant ribozymes could arise from an increase in the probability of docking in the incorrect registers or from faster cleavage once docked in the incorrect registers. Because the mutations have only a small effect on the rate of the chemical step for cleavage of S at the correct site, decreasing k_c by $\sim$2-fold (Young et al., 1991), and because the same active site appears to be used for the correct and incorrect cleavages, it is unlikely that the infidelity results from faster cleavage by the mutant ribozymes subsequent to docking into the alternate registers. These data therefore suggest that the mutations in J1/2 cause infidelity by increasing the probability of docking in alternate registers.

The Cleavage Site Is Chosen after Binding. Substitution of sulfur for a nonbridging phosphoryl oxygen atom to give the R_P thio isomer at the normal cleavage site slows the chemical step for the wild-type and mutant ribozymes by 2-fold. In contrast, this substitution has no effect on $(k_{cat}/K_m)^S$, because this second-order rate constant for reaction of E·G with S is limited by binding of S and not the chemical step (Herschlag & Cech, 1990b; Herschlag et al., 1991; Young et al., 1991). Similarly, there is no rate effect from thio substitution on $(k_{cat}/K_m)^S$ for the −3A mutant ribozyme (Figure 4, inset). However, thio substitution changes the ratio of products from the −3A ribozyme (Figure 4), giving less formation of P and more formation of P' and P''.

In order to account for the thio effect on the ratio of products but not on the overall rate, different steps must determine the rate of the reaction and the product that is formed. This requirement is met by the model in Scheme IVA. Following initial binding, the E·G·S complex can react to give
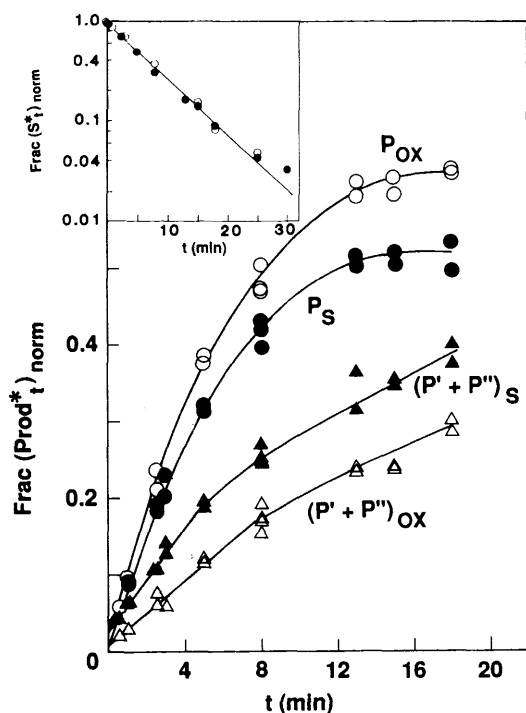
FIGURE 4: Thio effect on rate (inset) and products from cleavage of $G_2CCCUCUAGU$ (open symbols) and (R_P)-$G_2CCCUCU_{(P-S)}AGU$ (closed symbols) by the −3A ribozyme. Reactions were carried out with 40 nM −3A ribozyme, ∼1 nM 5′-end-labeled normal or thio-containing oligonucleotide substrate, and 800 μM G in the presence of 50 mM MES, pH 7, and 10 mM $MgCl_2$ at 50 °C. The inset shows the disappearance of $G_2CCCUCUAGU$ (open symbols) and (R_P)-$G_2CCCUCU_{(P-S)}AGU$ (closed symbols). The main figure shows the products that are formed in these reactions. The open circles correspond to P formed from the normal substrate ($G_2CCCUCUAGU$), and the open triangles correspond to the sum of P′ and P″ formed from this substrate. The closed circles and triangles correspond to P and to the sum of P′ and P″, respectively, formed from the thio substrate [(R_P)-$G_2CCCUCU_{(P-S)}AGU$]. (P, P′ and P″ are defined in Scheme I.) The ratio of P′ to P″ formed was unaffected by the thio substitution (<20% change in the ratio; data not shown). In the inset, the fraction of S* remaining at each time was normalized by subtracting the fraction of S* that did not react at long times ($fracS^*_{t→∞}$ = 0.05 for the normal substrate and 0.10 for the thio substrate) and then dividing by the fraction of S* that was reactive: i.e., $frac(S_t)_{norm} = (fracS^*_t - fracS^*_{t→∞})/(1 - fracS^*_{t→∞})$. Each time point is the average of two separate determinations. In the main figure, the fraction of each product at each time was normalized in the same way, by dividing by the fraction of S* that was reactive, so that at $t = ∞$ the sum of the product fractions is 1.0 [i.e., $frac(prod^*_t)_{norm}$ = $frac(prod^*_t)/(1 - fracS^*_{t→∞})$, with the values of $fracS^*_{t→∞}$ above].

P, P′, or P″. Even though there is a thio effect on the chemical step for formation of P (Young et al., 1991; this step is depicted with an asterisk in Scheme IV), there is no thio effect on the observed rate because binding of S is rate-limiting under the conditions of Figure 4 (Young et al., 1991). Despite the absence of an overall rate effect, the ratio of products from Scheme IVA can be changed by slowing the chemical step to form P but not the chemical step to form P′ and P″. No thio effect is expected in the formation of P′ and P″ because phosphate remains, rather than phosphorothioate, at the reactive linkages and phosphorothioate substitution one position 3′ to the normal cleavage site of S does not affect its cleavage by the wild-type ribozyme (J. A. Piccirilli and T. R. Cech, unpublished results). Thus, this thio substitution is expected to decrease the amount of P formed and correspondingly increase the amount of P′ and P″ formed. This is indeed observed: the initial slopes in Figure 4B show that the ratio of $[P/(P' + P'')]$ decreases from 4.2 to 2.1 upon thio substitution. The ratio of these ratios gives the thio effect of k_c^{ox}/k_c^{thio} =

Scheme V
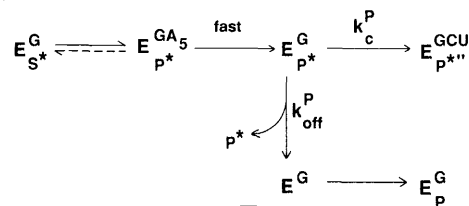
2.0 on the chemical step, according to eq 2, which was derived from Scheme IVA and eqs 1a and 1b. This calculated thio effect is consistent with the thio effect of 1.7 obtained directly under conditions that render the chemical step rate-limiting (Young et al., 1991).

$$R^{ox} = [P/(P' + P'')] = k_c^{ox}/(k_c' + k_c'') \qquad (1a)$$

$$R^{thio} = [P/(P' + P'')] = k_c^{thio}/(k_c' + k_c'') \qquad (1b)$$

$$\text{thio effect} = k_c^{ox}/k_c^{thio} = R^{ox}/R^{thio} \qquad (2)$$

In contrast to the ability of Scheme IVA to account for the change in product ratios upon thio substitution that occurs without a thio effect on the overall rate, the alternative model of Scheme IVB cannot account for these data. In Scheme IVB there are three forms of the ribozyme without bound S: E·G reacts with S to give P, E′·G reacts to give P′, and E′·G reacts to gives P″. However, this model does not provide different rate- and product-limiting steps. After rate-limiting binding, the ribozyme cannot "choose" where to cleave the substrate so that the thio substitution cannot change the product ratio. The inadequacy of Scheme IVB is also demonstrated by the observed increase in the rate of formation of P′ and P″ upon thio substitution (Figure 4, initial slopes); in model B this rate is expected to be unaffected by thio substitution.

Thus, as depicted in Scheme IVA, the ribozyme can choose a cleavage site after binding the substrate. This finding foreshadowed the ability of a mutant ribozyme to act processively, cleaving at one site and then another without releasing the intermediate between cleavages, as is described in the following section.

The +2A Ribozyme Cleaves RNA Processively. The ability to choose a cleavage site after binding of S (Scheme IVA) raises the possibility that, following an initial cleavage, there could be a second cleavage without dissociation of the first product. This is depicted in the top line of Scheme V. Processivity requires (1) multiple binding modes to place different phosphodiester bonds in the active site, (2) a pathway for changing binding modes without dissociating, and (3) a rate constant for the subsequent chemical step to form the shorter product that is faster than the rate constant for dissociation of P, the initial product (Scheme V, $k_c^P > k_{off}^P$). Multiple binding modes (1) via alternate docking of the P1 helix were demonstrated above. In addition, a pathway for changing binding modes without dissociating (2) was demonstrated in the previous section by the ability of the −3A ribozyme to choose the site of cleavage subsequent to binding the substrate. Finally, the values of k_c^P = ∼6 min⁻¹ (Table I) and k_{off}^P = ∼1 min⁻¹ (Young et al., 1991) for the +2A ribozyme (50 °C, 50 mM MES, pH 7, and 10 mM $MgCl_2$) suggest that the final criterion for processivity is met by this ribozyme.

Processivity was demonstrated for the +2A ribozyme by a pulse–chase experiment (Figure 5). This experiment was carried out at 30 °C rather than 50 °C to slow the reaction so that the first cleavage of S* to give P* could be distinguished from the second cleavage of P* to give (predominantly) P*″.
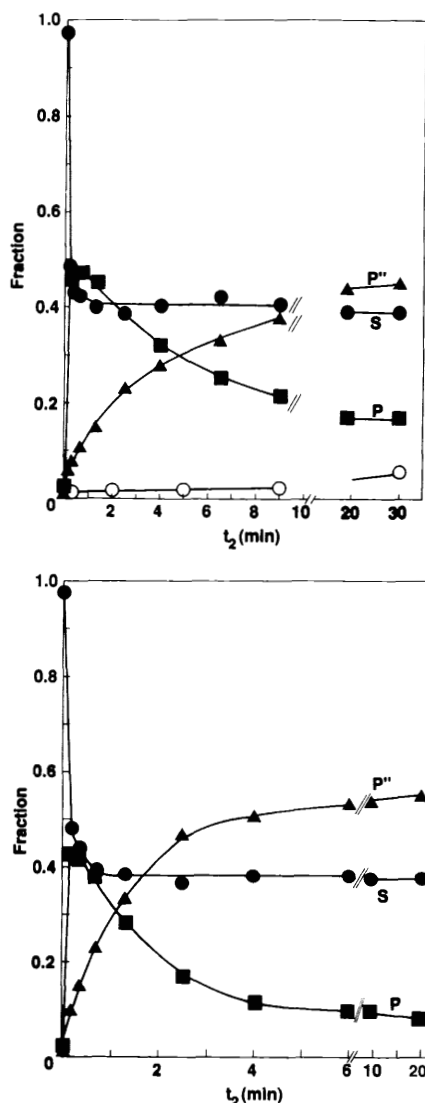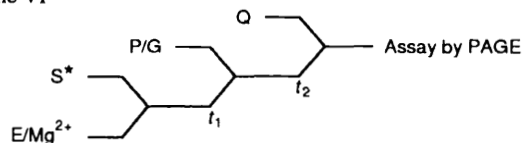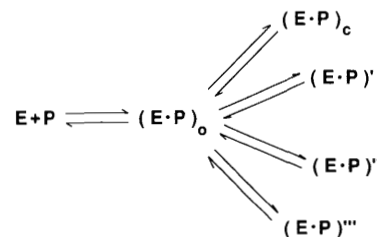
Scheme VII

proceed to form P*''. As seen in Figure 5, S* disappears very quickly, forming predominantly P*. Subsequently this P* disappears, reacting to give P*''. The absence of P*'' formation from P* when P* is added at t_2 with the chase (Figure 5A, open symbols) shows that only P* that remains bound to the ribozyme can proceed to give P*''. Thus, there is processivity of 70% at pH 7.0 (Figure 5A) and 85% at pH 7.9 (Figure 5B).

The rate constants $k_c^P = 0.2$ and 0.6 min^{-1} at pH 7.0 and 7.9, respectively (30 °C, 10 mM MgCl$_2$), and $k_{off}^P = 0.1$ min^{-1} at both pH values (k_c^P and k_{off}^P are defined in Scheme V) were determined from the rate constant and extent of P*'' formation in Figure 5, following the calculations described previously (Herschlag & Cech, 1990b). These data are consistent with a direct measurement that gave the same value of $k_c^P = 0.2$ min^{-1} [10 nM +2A ribozyme (saturating), ~1 nM P*, and 2.0 mM G with 50 mM MES, pH 7.0, and 10 mM MgCl$_2$ at 30 °C; data not shown]. Independent experiments provided evidence for an increase in the rate constant for the chemical step with increasing pH without an effect on the affinity for P (data not shown), again consistent with the results from Figure 5. Processivity was also observed at 50 °C, with 0.17, 0.47, and 0.70 of the P* forming P*'' at pH 6.1, 7.0, and 7.9, respectively (in 2 mM G and 10 mM MgCl$_2$); however, the faster reactions at the higher temperature rendered it more difficult to observe the successive accumulation and disappearance of P* that is clearly distinct in Figure 5.

Evidence for Two-Step Binding of Oligonucleotides to the Ribozyme and Relative Energetic Barriers. Our understanding of the formation of the P1 duplex between an RNA oligonucleotide, S or P, and the 5' exon binding site of the ribozyme has been refined by the experiments described in this section. They provide evidence for an (E·S)$_o$ or (E·P)$_o$ "open" complex, in which the P1 duplex has formed, and an (E·S)$_c$ or (E·P)$_c$ "closed" complex, in which the P1 helix has docked into tertiary interactions with the ribozyme.

Consider the processive reaction catalyzed by the +2A ribozyme. After cleavage of S, P is bound in the active site with a tertiary contact to the 2'-hydroxyl of the −3 residue. However, for the subsequent cleavage to give P'', the tertiary interaction with the 2'-hydroxyl of residue −3 must be broken and the −3 residue must be replaced by the −5 residue in this tertiary contact (see above). If binding occurred with only one significant energetic barrier, then, by microscopic reversibility, breaking the tertiary contact would result directly in dissociation and there would be no processivity. In other words, any time the tertiary interactions were broken, the duplex would also fall apart. Thus, an energetic barrier in addition to that for breaking the tertiary interactions is required to prevent the oligonucleotide from falling off and thereby allow processivity. This is depicted in the two-step binding mechanism of Scheme VII and Figure 6. (E·P)$_c$, which contains the P1 helix in its normal register after cleavage of S, could break its tertiary contacts without dissociating to give the open complex, (E·P)$_o$. The P1 helix in this open complex could then reenter a closed complex, by docking into the tertiary interactions, to give, for example, (E·P)'', which is the binding

FIGURE 5: Processivity of the +2A ribozyme. The +2A ribozyme (300 nM) and ~1 nM S* (p*G$_2$CCCUCUA$_5$) were incubated at 30 °C in 50 mM MES, pH 7.0, and 10 mM MgCl$_2$ for t_1 = 1 min, followed by a 10-fold dilution at t_2 = 0 with a chase solution to give the following final concentrations: 2.0 mM G, 2 μM unlabeled P, 10 mM MgCl$_2$, and 50 mM MES, pH 7.0 (top panel) or 50 mM HEPPS, pH 7.9 (bottom panel). The time course following the chase is shown, with ● representing S*, ■ representing P*, and ▲ representing P*''. The open symbols in the top panel represent the results of a control experiment that was analogous to the experiment described except that S* was omitted and P* was added at t_2 = 0 along with the G and unlabeled P. The ribozyme was preincubated at 50 °C for 20 min in 75 mM MES, pH 7.0, and 15 mM MgCl$_2$. This renaturation treatment is required to allow the ribozyme to adopt its active conformation (D.H. and P. Legault, unpublished results). Experiments in which the ribozyme concentration was decreased 3-fold still gave reaction of ~60% of the initial S*, as in this figure. These and other data (D.H. and P. Legault, unpublished observations) suggest that the unreactive S* can form a tight complex with ribozyme that is sequestered in an inactive conformation.

Scheme VI

As outlined in Scheme VI, the E·S* complex is first formed during t_1; at t_2 = 0 there is a simultaneous addition of G, which allows the reaction to start, and unlabeled P, which prevents the rebinding of P* so that only P* remaining bound can
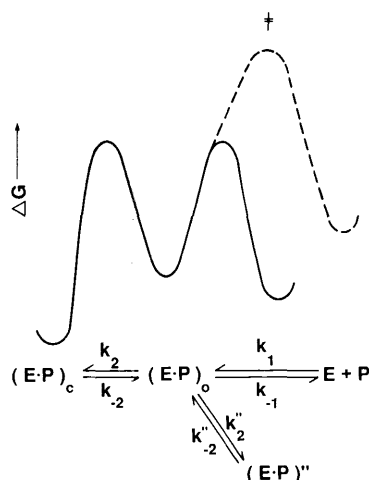
FIGURE 6: Qualitative free energy–reaction profile for the two-step binding model, depicted in the direction of dissociation, for the conditions $[P] > K_d(E \cdot P)$. E is the ribozyme and P is the oligonucleotide that forms a perfect duplex with the 5' exon binding site (Figure 1 and Scheme I). $(E \cdot P)_c$ and $(E \cdot P)''$ are closed conformations in which the tertiary contacts are made, whereas $(E \cdot P)_o$ is the open conformation, in which P is held solely by base pairing, with no tertiary interactions. $(E \cdot P)_c$ represents binding in the normal docking mode, which is the alignment directly following cleavage of E·S to form E·P (i.e., with the predominant tertiary interaction to the 2'-hydroxyl at position –3); $(E \cdot P)''$ represents binding in the docking mode that gives cleavage to product P'' (i.e., with the tertiary interactions displaced such that the contact to the 2'-hydroxyl of residue –3 has been replaced by a contact to the 2'-hydroxyl of residue –5; Scheme II). ‡ represents the highest free energy barrier and therefore the barrier for the rate-limiting step. The free energy values for individual species and transition states will vary for the wild-type and mutant ribozymes and have not all been measured; estimates for some of the rate constants are described under Further Discussion.

register for the reaction that gives P''. Furthermore, in order to have efficient processivity, redocking of P into the $(E \cdot P)''$ complex must be favored over dissociation to give free E and P. This is depicted in Figure 6 by the higher energetic barrier for $(E \cdot P)_o \rightarrow E + P$ than for: $(E \cdot P)_o \rightarrow (E \cdot P)''$. The binding reaction, which is depicted by the reverse of the dissociation reaction of Figure 6 (i.e, from *right to left*), therefore has the first of the two binding steps rate-limiting.

The first binding step is presumably formation of the P1 helix without the tertiary interactions [i.e., $(E \cdot P)_o$ or $(E \cdot S)_o$; see below]. This first step of duplex formation is itself a multistep process that presumably involves nucleation of a few base pairs followed by zipping up of the helix [e.g., Porschke & Eigen, 1971; Craig et al., 1971; see also (2) below]. The second step may also be a multistep process, with several species both on and off the pathway of docking into the tertiary interactions that are separated by quite smaller energetic barriers. What is shown above is that there are at least two energetic barriers of mechanistic significance: the first barrier presumably determines how fast the oligonucleotide forms and breaks a duplex with the ribozyme, and the second barrier determines how fast the tertiary contacts between this P1 duplex and the ribozyme are formed and broken.

There is considerable additional evidence supporting this two-step binding model. (1) As described above, the occurrence of a thio effect on the product ratio, but not on the rate of reaction, shows that the cleavage site is chosen after binding to the –3A ribozyme. A minimal model with only one binding step was presented in Scheme IVA. However, since cleavage at different sites is accompanied by docking into the tertiary interactions in different registers, the –3A ribozyme·oligonucleotide complex must interconvert between tertiary interactions without dissociating. This provides the same type of

evidence for a two-step binding model as the processivity result with the +2A ribozyme. An additional barrier is required to prevent dissociation after the tertiary interactions are broken, as depicted in Scheme VII and Figure 6.

(2) The rate constant $k_{on} = \sim 10^8$ M^{-1} min^{-1} for binding of oligonucleotides to the wild-type ribozyme is of the order observed for duplex formation between two oligonucleotides in solution (Herschlag & Cech, 1990b; Turner et al., 1990). This is consistent with the two-step binding pathway as depicted in Figure 6, in which the first step of duplex formation is rate-limiting (i.e., essentially every time the duplex is formed, the RNA oligonucleotide then docks into the tertiary interactions rather than falling off).

(3) Despite the $\sim$15- and 150-fold weaker binding of RNA oligonucleotides caused by the +2A and –2A mutations, respectively, the rate constants for binding of oligonucleotides are the same, within experimental uncertainty (Young et al., 1991; small variations of $\sim$2-fold may arise from the presence of some inactive ribozyme or differences in accessibility of the 5' exon binding site). Thus, the strength of the tertiary interactions does not affect the rate constant for binding, consistent with rate-limiting duplex formation, as depicted in Figure 6.

(4) Binding of RNA oligonucleotides is weakened by $\sim$ 50-fold when Mg^{2+} is replaced by Ca^{2+}, suggesting that the tertiary interactions are weakened or absent (Pyle et al., 1990; T. S. McConnell, D.H., and T. R. Cech, unpublished results). However, the rate constant for binding is decreased by less than 2-fold (T. S. McConnell, D.H., and T. R. Cech, unpublished results). This is again consistent with binding that is limited by the rate of duplex formation, as depicted in Figure 6.

(5) The wild-type and mutant ribozymes form duplexes with deoxyribooligonucleotides that are much weaker than the duplexes with ribooligonucleotides (Herschlag & Cech, 1990a, Pyle et al., 1990; Pyle & Cech, 1991; Young et al., 1991). It is reasonable that DNA binds to the ribozyme in the open $(E \cdot P)_o$ conformation, which lacks the 2'-hydroxyl tertiary interactions.

Formation of Shorter Products from both S and P. The cleavage of P* to shorter products was demonstrated above (Figure 3A and Table I). However, when reactions are initiated with S, the formation of products shorter than P could arise solely from the recleavage of P or could arise additionally from the direct cleavage of S at the alternate positions. In order to test this, reactions were carried out with 3'-end-labeled oligonucleotide substrate, G$_2$CCCUCUAGUp*Cp. The normal cleavage gives GAGUp*Cp and unlabeled G$_2$CCCUCU. Thus, recleavage of the unlabeled 5' product would not give additional bands in PAGE, whereas direct cleavage of the substrate at alternate positions would result in additional bands. Slower migrating species were indeed observed in the reactions of the mutant ribozymes, consistent with direct cleavage at positions 5' of the normal cleavage site (data not shown). The absence of these additional species from cleavage by the wild-type ribozyme (data not shown) was consistent with the greater fidelity of the wild-type ribozyme. In addition, the preferred positions of the additional cleavages for each mutant ribozyme agreed with those determined by mapping of the 5' products using 5'-end-labeled substrate. The same results were obtained from analysis of cleavage of the oligonucleotide substrate 3'-end-labeled with cordycepin (these reactions were carried out with GTP replacing G so that the order of migration would follow the length of the oligonucleotide; data not shown).

Scheme VIII
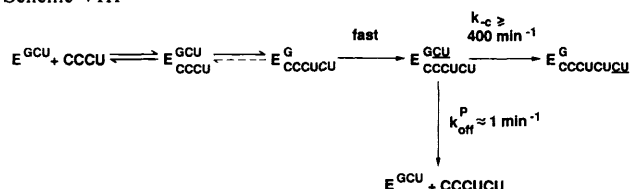
It was at first surprising that cleavage of S directly to the alternative products was observed, because the calculated rate of cleavage of S at the normal site of $k_c = \sim 400$ min^{-1} (Young et al., 1991) is much faster than the cleavage of P, with $k_c^P = \sim 5$ min^{-1} (Table I). Considerably more than 1% of the products from cleavage of S corresponded to the cleavage at the alternate positions. For example, the -3A ribozyme gave $\sim 25\%$ of the alternative products directly from S (see Figure 4). This suggests that the alternate cleavage of S is ~ 20-fold faster than that of P. That the (initial) alternate cleavage in Figure 4 arises predominantly from direct cleavage of S is demonstrated by the observation that the ratio of P'/P'' is >1 in this experiment (data not shown), whereas cleavage of P gives a ratio P'/P'' <1 (Table II; this change in ratio can be determined accurately because it is near 1). Thus, despite the similar values of K_d for S and P for the wild-type and mutant ribozymes (Herschlag & Cech, 1990b; Pyle et al., 1990), the different rate and positional preference of alternate cleavage shows that there are differences in their interactions in the active site.

FURTHER DISCUSSION

Processivity by Catalytic RNA. The discovery of catalytic RNA rendered a plausible solution to the "chicken and egg" problem of which came first: information storage (nucleic acid) or catalytic function (proteins), since RNA could have served both functions (e.g., Cech, 1986; Pace & Marsh, 1986). In an RNA world, an RNA enzyme would have needed to perform replication, via an RNA-dependent RNA polymerase activity. Szostak and co-workers have made remarkable progress in reengineering group I ribozymes to polymerize RNA with use of external templates (Doudna & Szostak, 1989; Doudna et al., 1991). An additional property desired for a polymerase is the ability to act processively, successively adding nucleotides without release of a growing RNA or DNA chain. Cellular RNA and DNA polymerases can add thousands of nucleotides without dissociation (e.g., O'Donnell & Kornberg, 1985, and references therein).

It was shown herein that an RNA enzyme can also act processively. Though the processivity is quite modest compared to that of some protein enzymes, this result nevertheless establishes that an RNA enzyme has the capacity to act processively. The results of Figure 5 demonstrated processivity for cleavage of an oligonucleotide, the reverse of the more pertinent polymerization reaction. Scheme VIII shows the reverse of the processive cleavage reactions, i.e., a polymerization reaction.[4] The ~ 400-fold faster rate of the chemical step (k_{-c}) compared to that of dissociation (k_{off}^P) indicates that the $+2$A ribozyme is also expected to exhibit processivity in polymerization and that this processivity is expected to be

much greater than in cleavage.[5]

An Induced Fit Conformational Change upon Binding of S. The 5' exon binding site, which forms a duplex with RNA oligonucleotides, and the functional groups of the ribozyme responsible for tertiary contacts are not positioned for binding of oligonucleotides in the free ribozyme. Rather, the P1 duplex between the 5' exon binding site and the oligonucleotide must undergo a conformational change to dock into the tertiary interactions (Figure 6 & Scheme VII). Thus, the second step in binding of the oligonucleotide, docking into the tertiary interactions, can be considered an induced fit conformational change (Koshland, 1958).

A simple induced-fit mechanism, in which the chemical step or another central step is rate-limiting, does not enhance specificity (Herschlag, 1988). However, there are several alternative mechanisms that allow a conformational change to provide specificity. One such alternative mechanism occurs when the enzyme surrounds the substrate on all sides, thereby providing greater interactions for catalysis and specificity but necessitating a conformational change to allow substrate binding. This type of conformational change appears to be common [e.g., references in Herschlag (1988)]. A second alternative mechanism can occur when substrate binding is rate-limiting, as for the *Tetrahymena* ribozyme. Young et al. (1991) have shown that the J1/2 mutations increase substrate specificity up to ~ 70-fold over that for the wild-type ribozyme. The mutations in J1/2 disrupt the positioning of the P1 duplex with respect to the tertiary interactions, thereby making the induced-fit conformational change less favorable. The free energy–reaction profiles of Figure 7 show that this induced-fit conformational change is responsible for the enhanced specificity.

Figure 7 shows a free energy–reaction profile for cleavage of a matched (S_M) and mismatched substrate (S_{MM}) by the ribozyme; S_M forms a perfect or matched duplex with the 5' exon binding site, and S_{MM} forms a duplex containing a single mismatch. There is little specificity for S_M, only ~ 10-fold, with the wild-type ribozyme, because binding is predominantly rate-limiting for both S_M and S_{MM} (Figure 7, wt). However, the -2A mutation increases specificity dramatically, to ~ 700-fold (500 μM GTP; Young et al., 1991). The increased specificity arises because the conformational change has become less favorable: $\Delta G'_{IF}$ for the -2A ribozyme is less negative than ΔG_{IF} for the wild-type ribozyme (Figure 7). This causes the chemical step to become rate-limiting for S_{MM}, while binding remains rate-limiting for S_M. This induced-fit mechanism is capable of providing specificity because rate-

---

[4] The 5' exon binding site of the ribozyme provides a template that is too short to base pair with the CU of the second GCU that is added in Scheme VIII, so that no significant specificity is expected for this addition. However, specificity does occur with longer template RNA that can base pair with the incoming bases (Doudna & Szostak, 1989).

---

[5] The value of $k_{off}^P = \sim 1$ min^{-1} is from Young et al. (1991; 50 °C). The estimate of $k_{-c} = \sim 400$ min^{-1} is a lower limit derived as follows. The overall equilibrium in the transesterification reaction (S + G $\rightleftharpoons$ P + GA$_5$) is near 1 (D.H. & T. S. McConnell, unpublished results). In addition, S and P bind similarly to the wild-type and -2A ribozymes (Herschlag & Cech, 1990b; Pyle et al., 1990), and presumably to the $+2$A ribozyme, so that the equilibrium for E·S + G $\rightleftharpoons$ E·P + GA$_5$ is also near 1. Experiments with the wild-type ribozyme suggested that GA (and presumably GA$_5$) binds no stronger than G, so that the equilibrium

$$\text{E·S·G} \underset{k_{-c}}{\overset{k_c}{\rightleftharpoons}} \text{E·P·GA}_5$$
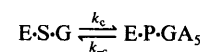
gives $K = (k_c/k_{-c}) \leq \sim 1$. Thus $k_{-c} \geq k_c = 400$ min^{-1} [the value of k_c is from Young et al. (1991)], and processivity of at least (400 min^{-1})/(400 min^{-1} + 1 min^{-1}) = 0.998 is expected. This calculation assumes that translocation of the substrate in the active site does not become rate-limiting; this assumption is supported by the data described under In The Two-Step Binding Mechanism, How Fast Does the P1 Duplex Dock and Undock?

wt

$$E_G + S \rightleftharpoons \left(E_G^S\right)_o \rightleftharpoons \left(E_G^S\right)_c \longrightarrow \text{products}$$

-2A

$$E_G + S \rightleftharpoons \left(E_G^S\right)_o \rightleftharpoons \left(E_G^S\right)_c \longrightarrow \text{products}$$
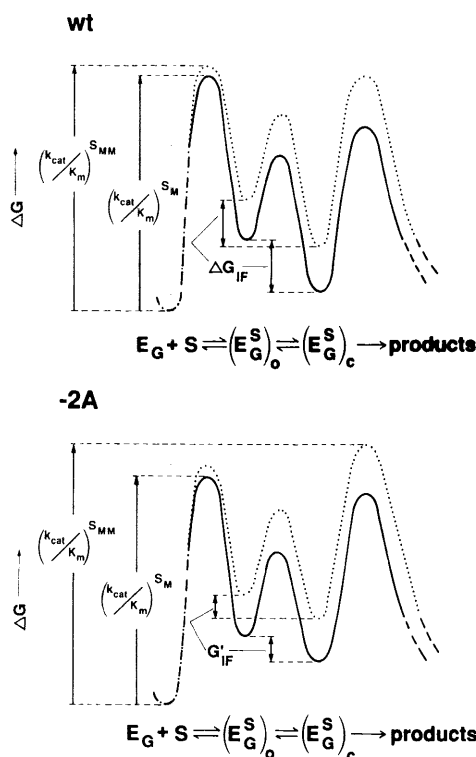
FIGURE 7: Free energy–reaction profiles for reactions of S_M (G_2CCCUCUA$_5$; solid line) and S_{MM} (G_2CCC$\underline{G}$CUA$_5$; dotted line) catalyzed by the wild-type (wt) and −2A ribozymes. S_M forms a matched or perfect duplex with the 5′ exon binding site, and S_{MM} forms a duplex with a G·A mismatch. The free energy profiles are drawn for k_{cat}/K_m conditions, with $[S_M]$ or $[S_{MM}] = 0.1$ nM [which is less than $K_d(E \cdot S_M)$ and $K_d(E \cdot S_{MM})$], $[G] \gg K_d^G$, and $[E] \ll [S_M]$ or $[S_{MM}]$. The ratio of k_{cat}/K_m values determines specificity under all conditions, whether S is subsaturating or saturating (Fersht, 1985). The −2A mutation renders the induced-fit conformational change of the open to closed complex less favorable ($\Delta G'_{1F}$ for the −2A ribozyme vs ΔG_{1F} for the wild-type ribozyme) but has no other significant effects on the free energy profiles. (The rate constant for the chemical step is decreased $\sim$2-fold.) The rate and equilibrium constants used in the profiles are described in Young et al. (1991) and are from that paper and Herschlag and Cech (1990b,c), except for the energies of the $(E \cdot G \cdot S)_o$ complexes. The values of $K_d(E \cdot S)_o = 10$ and 6800 μM for S_M and S_{MM}, respectively, were calculated from nearest neighbor rules for simple duplexes (Freier et al., 1986) as described in Herschlag and Cech (1990c). The same values of $K_d(E \cdot S)_o$ were used for the wild-type and −2A ribozymes, as this complex represents simple duplex formation (see text) and these ribozymes bind DNA oligonucleotides with essentially the same affinity (Young et al., 1991). A rate constant of 10^5 min^{-1} for conversion of $K_d(E \cdot S)_o$ to $K_d(E \cdot S)_c$ was assumed (see In the Two-Step Binding Mechanism, How Fast Does the P1 Duplex Dock and Undock?). It should be noted that the free energy profiles are calculated for saturating G but that the observed specificity values given in the text were obtained with 500 μM GTP rather than with saturating GTP or G [$K_d(E \cdot G) = \sim 1$ mM for the wild type and ~ 4 mM for the −2A ribozyme; see Young et al. (1991)]. There is evidence for (nearly) independent binding of S and G (Herschlag & Cech, 1990b) so that determination of the analogous free energy–reaction profile with subsaturating G is straightforward.

limiting binding of S_M allows the conformational change to slow the reaction of S_{MM} but not that of S_M.

In the Two-Step Binding Mechanism, How Fast Does the P1 Duplex Dock and Undock? Evidence suggesting two significant energetic barriers in the binding of oligonucleotides was presented above (Figure 6 and Scheme VII). Further data suggested that the first binding step is formation of the P1 duplex between an RNA oligonucleotide and the 5′ exon binding site of the ribozyme (Figure 1) and the second binding step is docking of P1 into its tertiary interactions with the ribozyme. In this section, minimum estimates for the rate of docking and undocking in the second step are calculated (k_2

and k_{-2}, respectively, in Figure 6). The calculations suggest that this conformational rearrangement can be quite fast, with a minimum *estimate* of the rate constant for docking of $k_2 \geq 80\,000$ min^{-1} for the −3A ribozyme.

These calculations necessitate assumption of an equilibrium constant for formation of the initial open complex, $(E \cdot P)_o$. A reasonable estimate can be obtained if this initial complex is stabilized only by base pairing and not by tertiary interactions. The stability of this duplex, between the 5′ exon binding site of the ribozyme and the complementary oligonucleotide (P), is calculated by nearest neighbor rules to be $K_d = 10$ μM [50 °C; see Herschlag and Cech (1990c) and Freier et al. (1986) for calculation]; this is similar to the value of $K_d = 20$ μM for the duplex between the ribozyme and the complementary deoxyribooligonucleotide, which lacks the 2′-hydroxyl moieties that partake in the tertiary interactions (Herschlag & Cech, 1990a).[6]

The estimate of $K_d(E \cdot P)_o = 10$ μM, the measured value of $k_{on} = \sim 10^8$ M^{-1} min^{-1} for the wild-type and mutant ribozymes (Herschlag & Cech, 1990b; Young et al., 1991), and use of the conclusion that k_1 is rate-limiting for binding (Figure 6 and above) give $k_1 = k_{on} = \sim 10^8$ M^{-1} min^{-1} and $k_{-1} = [K_d \cdot (E \cdot P)_o](k_1) = (10$ μM$)(10^8$ M^{-1} min$^{-1}) = 1000$ min^{-1}. Since docking is not rate-limiting in binding, k_2 is larger than k_{-1} [i.e., after formation of $(E \cdot P)_o$, docking to give $(E \cdot P)_c$ is favored over dissociation to give $E + P$], and an estimate of $k_2 > 1000$ min^{-1} is obtained. For the +2A ribozyme, the processivity of 70% (pH 7.9, 50 °C, 10 mM MgCl$_2$) shows that $(E \cdot P)_o$ must partition at least 0.7 of the time to give $(E \cdot P)''$ rather than to free E and P so that $0.7 = k_2''/(k_2'' + k_{-1})$ allows a lower limit for k_2'' (k_2'' is the rate constant for docking in the position that gives cleavage of P to form P''; Figure 6). This equation and the estimate of $k_{-1} = 1000$ min^{-1} described above give $k_2'' \geq 2000$ min^{-1}.

A second approach using data for the −3A ribozyme provides minimum estimates for the rates of docking and undocking. The thio effect on the ratio of products from the −3A ribozyme showed that the ribozyme chooses its cleavage site after the substrate is bound, as described above. The chemical step for reaction of the −3A ribozyme occurs with a calculated rate constant of ~ 100 min^{-1} under the conditions of Figure 4 (Young et al., 1991; note that the 800 μM G is not saturating for binding since $K_d(E \cdot G) = \sim 4$ mM). Since the ribozyme chooses its site before the chemical step, the E·G·S complex must have time to dock and undock before the chemical cleavage, i.e., faster than 100 min^{-1}. A rough minimum of $k_{-2} = \sim 400$ min^{-1} for undocking would allow such equilibration prior to the reaction. In addition, it is estimated that the E·S closed complex is ~ 200-fold more stable than the open complex for the −3A ribozyme ($K_2 = k_{-2}/k_2 = \sim 1/200$; Figure 6).[7] These values of k_{-2} and K_2 give a minimum

---

[6] The following data suggest a minimum estimate of $K_d(E \cdot P)_o = 0.1$ μM: (1) $K_d = 0.15$ μM for binding of P to the −2A ribozyme; this binding might be expected to be at least as strong as that for simple duplex formation. It should be noted that the value of $k_{on} = \sim 10^8$ M^{-1} min^{-1} for the −2A ribozyme provides no indication of an inactive conformer, which could decrease the binding affinity as occurs with the −3A mutation (Young et al., 1991). (2) $K_d = 0.1$ μM for binding of S to the Ca^{2+} form of the wild-type ribozyme similarly provides a lower limit for $K_d(E \cdot S)_o$ (T. S. McConnell, D.H., and T. R. Cech, unpublished results; note that S and P RNA and DNA oligonucleotides bind with similar affinity in the presence of Mg^{2+}; Herschlag & Cech, 1990a,b). In the calculations in the text the rough estimate of $K_d(E \cdot P)_o = 10$ μM is used.

estimate for the rate constant for docking of $k_2 > 80\,000$ min^{-1} [$k_2 = k_{-2}/K_2 > 400$ min$^{-1}/(1/200) = 80\,000$ min^{-1}]. There are no data that would suggest whether the effect of the J1/2 mutations on binding of RNA oligonucleotides is expressed in k_2 or k_{-2}.

Structure–Function Implications. J1/2 is not conserved in length or sequence among group I introns (Michel & Westhof, 1990; Young et al., 1991). Considering this alone, one might have initially thought that if this sequence plays any role, it might act as a tether, allowing the P1 helix to reach the active site in the catalytic core (Figure 2). However, the −3A and −2A ribozymes cleave bound P as fast as the +2A ribozyme and faster than the wild-type ribozyme, despite the shorter J1/2 sequence of the −3A and −2A ribozymes. Furthermore, the transition-state stabilization for formation of P‴ [Table I, $k_c'''/K_d(\text{E·P})$] first decreases as J1/2 is shortened from 5 to 3, consistent with a tether effect, but instead of continuing to decrease as J1/2 is further shortened the stabilization increases as the length of J1/2 goes from 3 to 1. Thus, in the wild-type ribozyme J1/2 appears to have a structural role more integral than that of a simple tether.

If J1/2 is not acting as a simple tether, what then is the structural basis for the effects of the J1/2 mutations? These mutations have a large effect of up to ~1000-fold on the binding of the RNA oligonucleotide but only a modest effect of ~4-fold on the binding of guanosine (Young et al., 1991). It is often tempting to propose that a residue or sequence which predominantly affects the binding of one of two substrates directly interacts with that substrate. However, the observation that the specific tertiary interactions with two of the oligonucleotide 2′-hydroxyl groups are maintained, though weakened in net energy, upon removal of all three residues of J1/2 strongly suggests that the role of J1/2 in oligonucleotide binding is indirect rather than direct. RNA oligonucleotides, but not DNA oligonucleotides, bind much more weakly to the −2A and −3A ribozymes than to the wild-type ribozyme [Table I, $K_d(\text{E·P})$; $K_d(\text{E·dP})$ values for DNA oligonucleotides are from Young et al. (1991)], and bound P is cleaved ~600-fold slower by the wild-type than the mutant ribozyme (Table I, k_c^{P}). These effects of the mutations suggest that the wild-type J1/2 positions the P1 helix for docking of P1 correctly into the tertiary interactions (the maximum binding energy [$K_d(\text{E·P})$, Table I] and the maximum transition-state stabilization for correct cleavage of S [$k_c^{S}/K_d(\text{E·S})$, Young et al. 1991] occur with the wild-type ribozyme). It is difficult to imagine J1/2 exerting this effect solely through self-structure of the AAA sequence. Thus, an interaction of J1/2 with another portion of the ribozyme is suggested. It is however, generally difficult to distinguish between effects from favorable energetic contributions in the wild type and unfavorable conditions introduced by mutation (e.g., see Herschlag & Jencks, 1990).

The simplest expectation for the ribozymes with mutations in J1/2 would be that they would behave quite similarly, because they all lack the wild-type J1/2 sequence, which might

uniquely partake in a tertiary interaction with other residues of the ribozyme. However, the data of Table I present a more complex picture. For example, the transition-state stabilization for the alternate reactions for the −2A ribozyme follows the order $k''/K_d(\text{E·P}) > k'''/K_d(\text{E·P}) > k'/K_d(\text{E·P})$, which is different than the order followed for the −3A ribozyme, $k''/K_d(\text{E·P}) > k'/K_d(\text{E·P}) > k'''/K_d(\text{E·P})$. In addition, the energetic differences in the alternative cleavage reactions of the mutant ribozymes can be quite large, with differences of at least ~3 kcal/mol between the −2A and +2A or −3A ribozymes in the formation of P′ [$k_c'/K_d(\text{E·P})$].[8] Thus, there are energetically significant interactions that vary with the J1/2 mutation and the docking register which are not explained in direction or magnitude by simple length effects.

It is possible that these effects result from fortuitous additional interactions or "promiscuity" in RNA/RNA interactions. Promiscuity refers to the multiple possibilities for the folding of an RNA molecule that often appear to result in a distribution of RNA structures that are accessible in solution. This can be contrasted to the folding of proteins, which in general adopt a single overall structure. Structural promiscuity of the *Tetrahymena* ribozyme is suggested by the multiplicity of circularization reactions of full-length and truncated ribozymes (Zaug et al., 1985; Joyce & Inoue, 1987) and the ability to use different internal guide sequences in circularization reactions (Been & Cech, 1987). In addition, the guanosine exchange reaction, pGpN + G → pG + GpN, provides evidence for a second guanosine binding site on the ribozyme (Kay et al., 1988) that appears to not be used in the physiological splicing reaction (Michel et al., 1990; Been & Perrotta, 1991) and suggests that there may be several ways for a nucleoside to interact with and bind to an RNA surface. Similarly, it is possible that the mutant J1/2 and surrounding sequences might interact with areas on the ribozyme that the wild-type J1/2 does not contact. Indeed, there could be different interactions for a single mutant depending upon the register in which P1 docks into the tertiary interactions.

What Determines 5′ Splice Site Selection and Its Fidelity? Phylogenetic comparisons have revealed that group I introns almost invariably splice following a U residue at the 3′ end of the 5′ exon and that this U residue occurs opposite a G residue of the 5′ exon binding site in the P1 helix. Mutagenesis experiments have also shown that this G·U pair is important in the rate and fidelity of splicing (Barfod & Cech, 1989; Doudna et al., 1989). Doudna et al. (1989) varied the position of the G·U pair within each of four P1 helices of different length. Reactivity was generally highest when the G·U pair was in the range or "window" of 4–6 base pairs from the base of the helix, suggesting that this positioning can play a role in choosing the splice site. However, as P1 was lengthened, the preferred positions for the G·U pair were biased toward positions further from the base of P1. With the longest P1 studied, cleavage at G·U at position 7, outside of the window, was favored over cleavage at G·U at position 4. These data suggest that "measuring" from the base of P1 is not the sole determinant of 5′ splice-site selection in this region, perhaps due to tertiary interactions with L1, the loop at the end of the P1 helix, or with the end of the helix connected by L1.

---

[7] Although the observed value of $K_d(\text{E·P}) = 1$ μM, there is evidence that only ~$1/20$ of this ribozyme is in a conformation that can bind P (Young et al., 1991). Thus, the dissociation constant for binding to the active conformation is ~1 μM/20 = 50 nM. Using this value for $K_d(\text{E·P})$ and $K_d(\text{E·P})_o = 10$ μM to solve for K_2 (= k_{-2}/k_2; Figure 6), according to the equation $K_d(\text{E·P}) = [K_d(\text{E·P})_o](K_2)$, gives $K_2 = 1/200$; i.e., the (E·P)$_c$ complex is favored by ~200-fold over (E·P)$_o$. The values of K_d observed for binding of S and P are similar for the wild-type ribozyme (Herschlag & Cech, 1990b) and for the −2A ribozyme (Pyle et al., 1990), and there is evidence that this is also the case for the −3A ribozyme (Young et al., 1991). The value of $K_2 = 1/200$, which was derived from K_d for binding of P, is therefore used in the text to determine k_s for docking of S.

[8] Table I lists the observed values for the transition-state stabilization relative to ribozyme, with bound G, and free oligonucleotide [i.e., $k_c'/K_d(\text{E·P})$, etc.]. However, there is evidence that only $1/20$ of the −3A ribozyme exists in an active conformation (Young et al., 1991). Thus, in calculating the energetic comparison for the −3A ribozyme a corrected value of $k_c'/K_d(\text{E·P})$ was used in order to obtain the transition-state stabilization relative to the free ribozyme in the active conformation: $k_c'/K_d(\text{E·P})^{\text{corrected}} = k_c'/K_d(\text{E·P}) \times 20$.

There is evidence that additional factors contribute to the fidelity of 5′ splice-site selection: even with the G·U pair appropriately positioned within P1, the data herein show that the length of J1/2 affects fidelity; mutations at positions 57 and 95 also decrease fidelity in the self-splicing reaction (W. Downs and T. R. Cech, personal communication). There is certainly no reason to believe that all of the positions that affect fidelity have been discovered. Thus, the alignment of P1 appears to involve several interactions. Multiple contacts may be required for correct positioning because of the many degrees of freedom of the RNA backbone or because the interactions are individually weak. It will be interesting to determine the additivity of mutational effects on RNA stability, binding, and catalysis.

Implications for Self-Splicing. The effects of the J1/2 mutations suggest that the structure involving J1/2 is functionally important in the efficiency and accuracy of the biological self-splicing reaction. The tight binding to the 5′ exon, for which the correct J1/2 is required, appears to prevent dissociation of the 5′ exon after the first step of self-splicing, thereby ensuring efficient exon ligation (Figure 1A; Herschlag & Cech, 1990c; see also Danenberg et al., 1989). The ~600-fold greater fidelity of the wild-type ribozyme than the mutant ribozymes (k_c^P, Table I) suggests that the wild-type J1/2 should minimize choice of an incorrect 5′ splice site, thereby ensuring accurate self-splicing.

Implications of Two-Step Binding and Alternate Docking for Other RNA-Mediated Processes. The results herein show a rearrangement of an RNA tertiary structure within a bound complex and provide a crude structural picture for this rearrangement. An RNA element, the P1 helix, can dock into RNA interactions in different registers, with the configuration within each binding register proper for catalysis. Analogous rearrangements of RNA elements may occur in other RNA-mediated processes, perhaps even with the same molecular strategies as employed in P1 docking: for example, in RNA-mediated splicing, allowing exit of the 5′ end of an intron from the active site and entry of the 3′ splice site; in pre-mRNA splicing, allowing a search for mRNA splice sites within a spliceosome and conferring a potential to choose between alternate splice sites (e.g., Goguel et al., 1991); in translation, allowing a search for a translation start site after initial recognition by the Shine–Dalgarno sequence, allowing motion of a ribosome along mRNA, and allowing a search for alternate codon–anticodon pairs to give translational frameshifting or hopping. In each case some RNA·RNA interactions are presumably maintained while others are made, broken, and remade. For example, in translational frameshifting and hopping, the peptidyl-tRNA is held in the P site while the codon–anticodon pairing is broken and re-formed elsewhere along the mRNA (Atkins et al., 1990).

As described above, the infidelity resulting from the mutations in J1/2 may be related to structural promiscuity of RNA. It may be that RNA is particularly suited to perform processes in which rearrangements between similar structures occur within bound complexes. Perhaps the role of proteins in these processes is to impose limits on and control RNA promiscuity, which unchecked would lead to infidelity. The proteins may act by favoring a particular structure through binding interactions (e.g., initiation factor's role in finding the initiation codon and initiator tRNA in translation; Hartz et al., 1989, 1990) and by proofreading (Thompson, 1988; Guthrie, 1991).

REFERENCES

Atkins, J. F., Weiss, R. B., & Gesteland, R. F. (1990) *Cell* 62, 413–423.

Barfod, E. T., & Cech, T. R. (1989) *Mol. Cell. Biol.* 9, 3657–3666.

Been, M. D., & Cech, T. R. (1987) *Cell* 50, 951–961.

Been, M. D., & Perrotta, A. T. (1991) *Science* 252, 434–437.

Cech, T. R. (1986) *Proc. Natl. Acad. Sci. U.S.A.* 83, 4360–4363.

Cech, T. R. (1990) *Annu. Rev. Biochem.* 59, 543–568.

Craig, M. E., Crothers, D. M., & Doty, P. (1971) *J. Mol. Biol.* 62, 383–401.

Danenberg, P. V., Shea, L. C. C., & Danenberg, K. (1989) *Biochemistry* 28, 6779–6785.

Davanloo, P., Rosenberg, A. H., Dunn, J. J., & Studier, F. W. (1984) *Proc. Natl. Acad. Sci. U.S.A.* 81, 2035–2039.

Doudna, J. A., & Szostak, J. W. (1989) *Nature* 339, 519–522.

Doudna, J. A., Cormack, B. P., & Szostak, J. W. (1989) *Proc. Natl. Acad. Sci. U.S.A.* 86, 7402–7406.

Doudna, J. A., Couture, S., & Szostak, J. W. (1991) *Science* 251, 1605–1608.

Downs, W. D., & Cech, T. R. (1990) *Biochemistry* 29, 5605–5613.

Fersht, A. (1985) *Enzyme Structure and Mechanism*, 2nd Ed., Freeman, New York.

Freier, S. M., Kierzek, R., Jaeger, J. A., Sugimoto, N., Caruthers, M. H., Neilson, T., & Turner, D. H. (1986) *Proc. Natl. Acad. Sci. U.S.A.* 83, 9373–9377.

Goguel, V., Liao, X., Rymond, B. C., & Rosbash, M. (1991) *Genes Dev.* 5, 1430–1438.

Good, N. E., Winget, G. D., Winter, W., Connolly, T. N., Izawa, S., & Singh, R. M. M. (1966) *Biochemistry* 5, 467–477.

Guthrie, C. (1991) *Science* 253, 157–163.

Hartz, D., McPheeters, D. S., & Gold, L. (1989) *Genes Dev.* 3, 1899–1912.

Hartz, D., Binkley, J., Hollingsworth, T., Gold, L. (1990) *Genes Dev.* 4, 1790–1800.

Herschlag, D. (1988) *Bioorg. Chem.* 16, 62–96.

Herschlag, D., & Cech, T. R. (1990a) *Nature* 344, 405–409.

Herschlag, D., & Cech, T. R. (1990b) *Biochemistry* 29, 10159–10171.

Herschlag, D., & Cech, T. R. (1990c) *Biochemistry* 29, 10172–10180.

Herschlag, D., & Jencks, W. J. (1990) *J. Am. Chem. Soc. 112*, 1942–1950.

Herschlag, D., Piccirilli, J. A., & Cech, T. R. (1991) *Biochemistry 30*, 4844–4854.

Joyce, G. F., & Inoue, T. (1987) *Nucleic Acids Res. 15*, 9825–9840.

Kay, P. S., Menzel, P., & Inoue, T. (1988) *EMBO J. 7*, 3531–3537.

Koshland, D. E., Jr. (1958) *Proc. Natl. Acad. Sci. U.S.A. 44*, 98–104.

Kruger, K., Grabowski, P. J., Zaug, A. J., Sands, J., Gottschling, D. E., & Cech, T. R. (1982) *Cell 31*, 147–157.

Latham, J. A., Zaug, A. J., & Cech, T. R. (1990) *Methods Enzymol. 181*, 558–569.

McSwiggen, J. A., & Cech, T. R. (1989) *Science 244*, 679–683.

Michel, F., & Westhof, E. (1990) *J. Mol. Biol. 216*, 585–610.

Michel, F., Hanna, M., Green, R., Bartel, D. P., & Szostak, J. W. (1989) *Nature 342*, 391–395.

O'Donnell, M. E., & Kornberg, A. (1985) *J. Biol. Chem. 260*, 12875–12883.

Pace, N. R., & Marsh, T. L. (1986) *Origins Life Evol. Biosphere 16*, 97–116.

Porschke, D., & Eigen, M. (1971) *J. Mol. Biol. 62*, 361–381.

Pyle, A. M., & Cech, T. R. (1991) *Nature 350*, 718–720.

Pyle, A. M., McSwiggen, J. A., & Cech, T. R. (1990) *Proc. Natl. Acad. Sci. U.S.A. 87*, 8187–8191.

Scaringe, S. A., Francklyn, C., & Ussman, N. (1990) *Nucleic Acids Res. 18*, 5433–5441.

Sugimoto, N., Sasaki, M., Kierzek, R., & Turner, D. H. (1989a) *Chem. Lett.*, 2223–2226.

Sugimoto, N., Tomka, M., Kierzek, R., Bevilacqua, P. C., &

Turner, D. H. (1989b) *Nucleic Acids Res. 17*, 355–371.

Tanner, N. K., & Cech, T. R. (1985) *Nucleic Acids Res. 13*, 7759–7779.

Thompson, R. C. (1988) *Trends Biochem. Sci. 13*, 91–93.

Turner, D. H., Sugimoto, N., & Freier, S. M. (1990) in *Nucleic Acids* Landolt–Bornstein Series, Vol. 1C, (Saenger, W., Ed.) Springer-Verlag, Berlin, pp 201–227.

Wu, T., Oglivie, K. K., & Pon, R. T. (1989) *Nucleic Acids Res. 17*, 3501–3517.

Young, B., Herschlag, D., & Cech, T. R. (1991) *Cell 67*, 1007–1019.

Zaug, A. J., & Cech, T. R. (1986) *Science 231*, 470–475.

Zaug, A. J., Grabowski, P. J., & Cech, T. R. (1983) *Nature 301*, 578–583.

Zaug, A. J., Kent, J. R., & Cech, T. R. (1985) *Biochemistry 24*, 6211–6218.

Zaug, A. J., Grosshans, C. A., & Cech, T. R. (1988) *Biochemistry 27*, 8924–8931.